

363 **A Proof of Theorem 1.2**

364 We now provide a rigorous proof of the result that was sketched in Section 2. This proof is essentially
 365 identical to [Deshpande et al., 2015, Lemma 4.4]. Recall the iterates (30) given by $\mathbf{s}^0 = \mathbf{x}^0 - \boldsymbol{\mu}^0 \odot \mathbf{x}^*$
 366 and

$$\mathbf{s}^{t+1} = \left(\frac{1}{\sqrt{N}\sqrt{\Delta}} \odot \mathbf{A} \right) f_t(\mathbf{s}^t + \boldsymbol{\mu}^t \odot \mathbf{x}^*) - \mathbf{b}_t \odot f_{t-1}(\mathbf{s}^{t-1} + \boldsymbol{\mu}^{t-1} \odot \mathbf{x}^*), \quad (43)$$

367 where $\boldsymbol{\mu}^t = (\mu_i^t)_{i \leq N}$ is given by the recursion

$$\mu_i^{t+1} = \mu_{g(i)}^{t+1} = \sum_{a \in [q]} \frac{c_a}{\Delta_{ag(i)}} \mathbb{E}_{x_0^*, Z} [x_0^* f_t^a(\mu_a^t x_0^* + \sigma_a^t Z)]$$

368 and $\mathbf{x}^* = (x_i^*)_{i \in [N]}$ is a vector with independent coordinates distributed according to \mathbb{P}_0 . By
 369 Lemma 2.4, for each $a \in [q]$, and any pseudo-Lipschitz function $\phi : \mathbb{R} \rightarrow \mathbb{R} \mapsto \mathbb{R}$ we have that
 370 almost surely

$$\lim_{N \rightarrow \infty} \frac{1}{|C_a^N|} \sum_{i \in C_a^N} \phi(s_i^t, x_i^*) = \mathbb{E}_{x_0^*, Z} \phi(\sigma_a^t Z, x_0^*) \quad (44)$$

371 where

$$(\sigma_b^{t+1})^2 := \sum_{a=1}^q \frac{c_a}{\Delta_{ab}} \mathbb{E}_Z [(f_t^b(Z_b^t))^2].$$

372 as was defined in (18). For any pseudo-Lipschitz function $\psi : \mathbb{R} \rightarrow \mathbb{R}$, we have $\phi(x, y) = \phi(x - \mu_a^t y)$
 373 is also pseudo-Lipschitz, so (44) implies that

$$\lim_{N \rightarrow \infty} \frac{1}{|C_a^N|} \sum_{i \in C_a^N} \psi(s_i^t + \mu_a^t x_i^*) = \mathbb{E}_{x_0^*, Z} \psi(\sigma_a^t Z + \mu_a^t x_0^*) \quad (45)$$

374 almost surely.

375 Now let $\hat{\mathbf{x}}^t$ be the iterates from the spiked AMP iteration for the inhomogeneous Wigner matrix (24)
 376 we derived in (26)

$$\mathbf{x}^{t+1} = \left(\frac{1}{N\Delta} \odot \mathbf{x}^* (\mathbf{x}^*)^T \right) \hat{\mathbf{x}}^t + \left(\frac{1}{\sqrt{N}\sqrt{\Delta}} \odot \mathbf{A} \right) \hat{\mathbf{x}}^t - \mathbf{b}_t \odot \hat{\mathbf{x}}^{t-1}. \quad (46)$$

377 It now suffices to show that for fixed t and all $a \in [q]$ that

$$\lim_{N \rightarrow \infty} \frac{1}{|C_a^N|} \sum_{i \in C_a^N} (\psi(s_i^t + \mu_a^t x_i^*) - \psi(x_i^t)) = 0 \quad (47)$$

378 almost surely. This will imply that $s_i^t + \mu_a^t x_i^*$ and x_i^t have the same asymptotic distribution which
 379 finish the proof of Theorem 1.2 by (45).

380 We now prove (47). Since ψ is L -pseudo-Lipschitz we have

$$\begin{aligned} |\psi(s_i^t + \mu_a^t x_i^*) - \psi(x_i^t)| &\leq L(1 + |s_i^t + \mu_a^t x_i^*| + |x_i^t|) |s_i^t + \mu_a^t x_i^* - x_i^t| \\ &\leq 2L |s_i^t + \mu_a^t x_i^* - x_i^t| (1 + |s_i^t + \mu_a^t x_i^*| + |s_i^t + \mu_a^t x_i^* - x_i^t|). \end{aligned}$$

381 The Cauchy–Schwarz inequality implies that

$$\begin{aligned} &\left| \frac{1}{|C_a^N|} \sum_{i \in C_a^N} (\psi(s_i^t + \mu_a^t x_i^*) - \psi(x_i^t)) \right| \\ &\leq \frac{2L}{C_a^N} (\sqrt{C_a^N} \|\mathbf{s}_a^t + \mu_a^t \mathbf{x}_a^* - \mathbf{x}_a^t\|_2 + \|\mathbf{s}_a^t + \mu_a^t \mathbf{x}_a^*\|_2 \|\mathbf{s}_a^t + \mu_a^t \mathbf{x}_a^* - \mathbf{x}_a^t\|_2 + \|\mathbf{s}_a^t + \mu_a^t \mathbf{x}_a^* - \mathbf{x}_a^t\|_2^2) \end{aligned}$$

382 where $\mathbf{s}_a^t = (s_i^t)_{i \in C_a^N} \in \mathbb{R}^{|C_a^N|}$, $\mathbf{x}_a^t = (x_i^t)_{i \in C_a^N} \in \mathbb{R}^{|C_a^N|}$. Therefore, to prove (47) it suffices to
 383 prove that for all $t \geq 0$,

$$\lim_{N \rightarrow \infty} \frac{1}{|C_a^N|} \|\mathbf{s}_a^t + \mu_a^t \mathbf{x}_a^* - \mathbf{x}_a^t\|_2^2 \rightarrow 0 \quad (48)$$

$$\limsup_{N \rightarrow \infty} \frac{1}{|C_a^N|} \|\mathbf{s}_a^t + \mu_a^t \mathbf{x}_a^*\|_2^2 \rightarrow 0 \quad (49)$$

384 Clearly, if we initialize $\mathbf{x}^0, \mathbf{s}^0$ at zero then (48) and (49) are satisfied by our state evolution equations
 385 (5). Notice that (49) follows directly from (45) applied to the square function. We use here that we
 386 assumed that the second moment of \mathbf{x}^* is finite.

387 We now focus on proving (48) through strong induction. By definition of the iterates (43) and (46),

$$\begin{aligned} & (\mathbf{s}_a^t + \mu_a^t \mathbf{x}_a^* - \mathbf{x}_a^t) \\ &= \left[\left(\frac{1}{\sqrt{N}\sqrt{\Delta}} \odot \mathbf{A} \right) f_{t-1}(\mathbf{s}^{t-1} + \boldsymbol{\mu}^{t-1} \odot \mathbf{x}^*) - \left(\frac{1}{\sqrt{N}\sqrt{\Delta}} \odot \mathbf{A} \right) f_{t-1}(\mathbf{x}^{t-1}) \right. \\ & \quad + \mu^t \odot \mathbf{x}^* - \left(\frac{1}{N\Delta} \odot \mathbf{x}^* (\mathbf{x}^*)^T \right) f_{t-1}(\mathbf{x}^{t-1}) \\ & \quad \left. + \mathbf{b}_{t-1}^x \odot f_{t-2}(\mathbf{x}^{t-2}) - \mathbf{b}_{t-1}^s \odot f_{t-2}(\mathbf{s}^{t-2} + \boldsymbol{\mu}^{t-2} \odot \mathbf{x}^*) \right]_{i \in C_a^N} \end{aligned}$$

388 where $[\cdot]_i$ corresponds to the i th row of a vector and \mathbf{b}_{t-1}^x and \mathbf{b}_t^s are the Onsager terms defined
 389 in (14) with respect to \mathbf{x}^{t-1} and \mathbf{s}^{t-1} respectively. The Cauchy–Schwarz inequality and Jensen’s
 390 inequality imply that there exists some universal constant C such that

$$\begin{aligned} & \frac{1}{|C_a^N|} \|\mathbf{s}_a^t + \mu_a^t \mathbf{x}_a^* - \mathbf{x}_a^t\|_2^2 \\ & \leq \frac{C}{|C_a^N|} \sum_{i \in C_a^N} \frac{1}{N} \left\| \left[\frac{1}{\sqrt{\Delta}} \odot \mathbf{A} \right]_i \right\|_2^2 \| [f_{t-1}(\mathbf{s}^{t-1} + \boldsymbol{\mu}^{t-1} \odot \mathbf{x}^*) - f_{t-1}(\mathbf{x}^{t-1})]_i \|_2^2 \\ & \quad + \frac{C}{|C_a^N|} \sum_{i \in C_a^N} \left(\mu_a^t - \left[\frac{1}{N\Delta} (f_{t-1}(\mathbf{x}^{t-1}) \odot \mathbf{x}^*) \right]_i \right)^2 (x_i^*)^2 \\ & \quad + \frac{C}{|C_a^N|} \sum_{i \in C_a^N} ([\mathbf{b}_{t-1}^x]_i - [\mathbf{b}_{t-1}^s]_i)^2 [f_{t-2}(\mathbf{s}^{t-2} + \boldsymbol{\mu}^{t-2} \odot \mathbf{x}^*)]_i^2 \\ & \quad + \frac{C}{|C_a^N|} \sum_{i \in C_a^N} [\mathbf{b}_{t-1}^x]_i^2 ([f_{t-2}(\mathbf{x}^{t-2})]_i - [f_{t-2}(\mathbf{s}^{t-2} + \boldsymbol{\mu}^{t-2} \odot \mathbf{x}^*)]_i)^2 \end{aligned}$$

391 We now control each term separately.

392 1. To control the first term, notice that the matrix $\frac{1}{N} \left[\frac{1}{\sqrt{\Delta}} \odot \mathbf{A} \right]$ has iid entries within blocks
 393 and the sizes of the blocks diverge with the dimension, so we can control the sums of the
 394 squares of within each block using standard operator norm bounds Anderson et al. [2010].
 395 The first term vanishes in the limit because f is pseudo-Lipschitz so we can apply the
 396 induction hypothesis bound which controls (48) at time $t - 1$.

397 2. To control the second term, notice that for $i \in C_a^N$ by Lemma 2.4 applied to the pseudo-
 398 Lipschitz function $y f_{t-1}(x)$ that

$$\left[\frac{1}{N\Delta} (f_{t-1}(\mathbf{x}^{t-1}) \odot \mathbf{x}^*) \right]_i \rightarrow \mu_a$$

399 almost surely. This implies that the average of such terms vanishes since we assumed that
 400 the second moment $\mathbb{E}[x_0^*]^2$ is finite.

401 3. To control the third and fourth terms, we can expand the definition of the Onsager terms
 402 and use the assumption that f' is pseudo-Lipschitz and almost surely bounded. Both terms
 403 vanish because our strong induction hypothesis gives us control of (48) at time $t - 2$.

404 Since all terms vanish in the limit, we have proven (48) for all $a \in [q]$, which finishes the proof of
 405 statement (47) and the proof of Theorem 1.2.

406 B Comparison with a naive PCA spectral method

407 In this appendix, we wish to show how the spectral method we propose differs, in practice, from a
 408 naive PCA. We provide an example of the spectrums of \mathbf{Y} and $\tilde{\mathbf{Y}}$ before and after the transition at

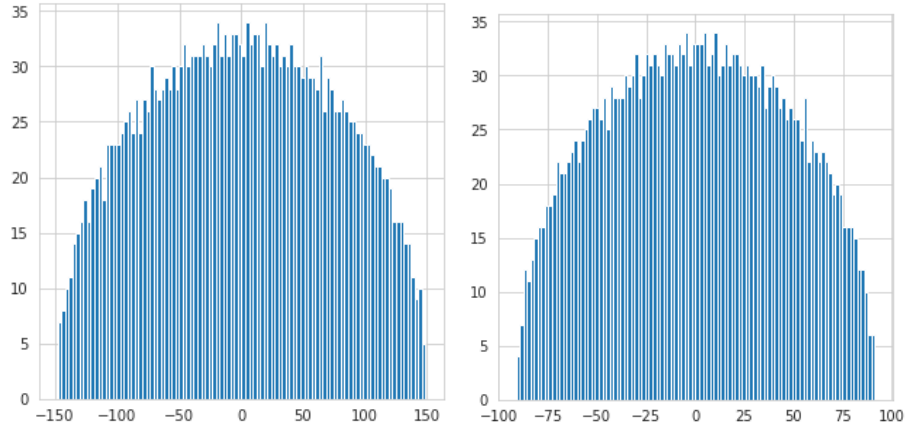


Figure 3: Illustration of the spectrum of $Y \in \mathbb{R}^{2500 \times 2500}$ evaluated at noise profiles with $\text{snr} \lambda(\Delta) = 0.7$ (left, before the transition) and on the left and 1.8 on the right (after the transition). There is no outlying eigenvalue in contrast to the transformed matrix: the transition for a naive spectral method is sub-optimal.

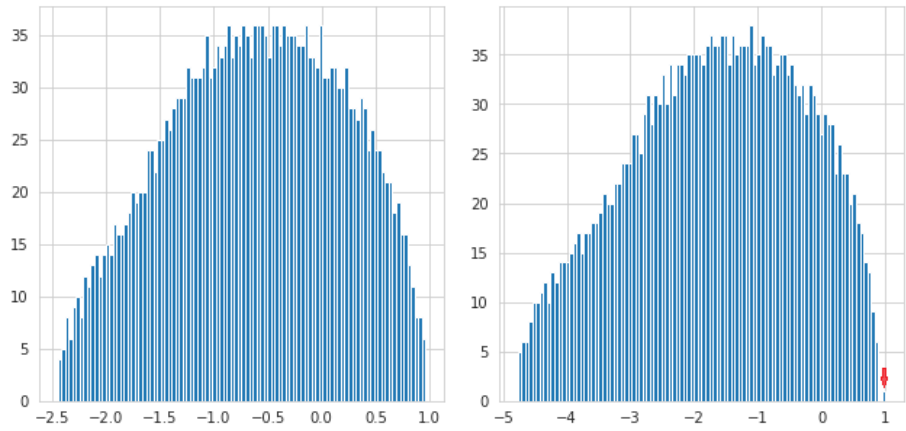


Figure 4: Illustration of the spectrum of $\tilde{Y} \in \mathbb{R}^{2500 \times 2500}$ evaluated at noise profiles with $\text{snr} \lambda(\Delta) = 0.7$ (left, before the transition) and on the left and 1.8 on the right (after the transition), with the outlying eigenvector correlated with the spike arises at eigenvalue one. This is at variance with the results of the naive method in Fig.3

409 $\text{SNR}(\Delta) = 1$. In Figure 3 there is no clear separation of the extremal eigenvalue of Y from the bulk
 410 around this transition. This is in contrast to Figure 4 where there is an extremal eigenvalue of \tilde{Y}
 411 appearing at value one.